Journal of Magnetic Resonance 255 (2015) 34–38

Contents lists available at ScienceDirect

Journal of Magnetic Resonance

journal homepage: www.elsevier.com/locate/jmr

Optimized selective lactate excitation with a refocused multiple-quantum filter

Mirjam Holbach [a,*], Jörg Lambert [b], Sören Johst [c], Mark E. Ladd [c,d], Dieter Suter [a]

[a] Experimental Physics III, TU Dortmund University, 44227 Dortmund, Germany
[b] Leibniz Institut für Analytische Wissenschaften – ISAS e.V., 44139 Dortmund, Germany
[c] Erwin L. Hahn Institute for Magnetic Resonance Imaging, University Duisburg-Essen, 45141 Essen, Germany
[d] Medical Physics in Radiology, German Cancer Research Center, 69120 Heidelberg, Germany

ARTICLE INFO

Article history:
Received 11 September 2014
Revised 20 February 2015
Available online 23 March 2015

Keywords:
Refocused SSel-MQC
Multiple-quantum filter
Lactate editing
MRS

ABSTRACT

Selective detection of lactate signals in *in vivo* MR spectroscopy with spectral editing techniques is necessary in situations where strong lipid or signals from other molecules overlap the desired lactate resonance in the spectrum. Several pulse sequences have been proposed for this task. The double-quantum filter SSel-MQC provides very good lipid and water signal suppression in a single scan. As a major drawback, it suffers from significant signal loss due to incomplete refocussing in situations where long evolution periods are required. Here we present a refocused version of the SSel-MQC technique that uses only one additional refocussing pulse and regains the full refocused lactate signal at the end of the sequence.

1. Introduction

Lactate is an important marker for anaerobic glucose metabolism, and the editing of lactate is therefore an important tool in cases such as cerebral ischemia, skeletal muscle disorders and in the supervision of therapy response in tumor treatment (see, e.g., [1]). The lactate methyl group signal is, however, often obscured by the intense lipid methylene signal around 1.3 ppm and cannot be resolved by conventional magnetic resonance techniques. As many tumors are located in areas where lipids are abundant or even contain lipids themselves, suppression of the lipid signal is mandatory to differentiate lactate resonances from the lipid signals. Various lactate editing techniques have been developed for this purpose. Among these, difference editing techniques and multiple-quantum filters use the differences in the scalar couplings in the molecules to excite the desired metabolites selectively and suppress other overlapping signals [2]. In difference editing techniques [3–6] two scans are acquired that are subtracted. Therefore, this method is substantially more sensitive to motion artifacts. The multiple-quantum lactate editing techniques (e.g. [7–10]) use magnetic field gradients to select multiple quantum coherences. They allow for a very high lipid suppression efficiency. As single-shot techniques they are relatively insensitive to motion artifacts.

Early work on selective excitation of lactate signals *in vivo* with multiple-quantum filters can be found e.g. in [11–13], where [11,12] represent double-quantum filters (DQF) and the work in [13] is based on a zero-quantum filter. The DQF investigated in this work is the sequence SSel-MQC from He et al. [7]. Current work on the basis of this spectral editing method is reported e.g. in [9,14–16,8,17,1,18–20]. Pickup et al. developed a combination of the Sel-MQC technique with longitudinal Hadamard slice selection and chemical shift imaging and facilitated the generation of lactate maps *in vivo* in selected regions [9]. The feasibility of the clinical application of this technique was demonstrated in [14]. In [15,1] it was shown that with this sequence the important application of monitoring of patient-specific markers of therapeutic response in cancer treatment is possible. In [16,17] the Sel-MQC sequence was implemented with fast spectrocopic imaging methods. For an inreased *in vivo* lactate signal the sequence was combined with binomial spectral selective pulses in [18]. Relaxation measurements were performed on the basis of the SSel-MQC sequence in [20].

A problem of the SSel-MQC sequence is the strong variation of the lactate signal with the length of the evolution period t_1 [7]. The signal is modulated with a factor $cos(\pi J t_1)$. A reliable lactate detection in an environment that is rich in lipids requires long evolution times t_1 to let the gradients dephase the lipid signal below the detection limit. In such situations this additional factor results in severe signal loss that can impede the detection of small lactate signals [8]. Moreover, half of the signal of the metabolite of interest

* Corresponding author. Fax: +49 2317553516.
E-mail address: mirjam.holbach@tu-dortmund.de (M. Holbach).

http://dx.doi.org/10.1016/j.jmr.2015.03.004
1090-7807/

is lost anyway due to the selection of the double-quantum coherences. Boer et al. suggest in [8] the use of two additional refocusing RF pulses to eliminate the signal modulation.

We present here a modified double-quantum lactate editing sequence which recovers the single-quantum inphase magnetization during the echo formation delay. The sequence shows no sensitivity to the choice of the echo delay, the length of which can be chosen according to the demands of lipid suppression. In contrast to the modification suggested by Boer et al. [8] to cope with the signal loss due to incomplete refocusing, the multiple-quantum evolution period in our sequence can be kept as short as in the original experiment of He et al. [7]. Moreover, our sequence requires only one instead of two additional 180° pulses.

2. Theory and pulse sequences

2.1. Selective multiple-quantum-coherence transfer (Sel-MQC)

The pulse sequence Sel-MQC, originally developed by He et al. [7], uses a double-quantum filter (DQF) for selective excitation of lactate methyl signals and simultaneous suppression of lipid and water signals in a single scan. Here we use the version SSel-MQC that refocuses the lactate methyl signals with a selective 180°-pulse in the evolution period (first delay t_1) of the sequence, as shown in Fig. 1. The magnetization of the J-coupled spins in the lactate molecules can be transformed to double-quantum coherences which pass the filter, while the spins in lipid and water molecules can only build single-quantum coherences, which are suppressed by the filter. The coherence selection gradients g_1 and g_2 refocus the lactate signal at the end of the sequence but dephase the signal from water and lipids.

The thermal equilibrium density operator of the lactate spins is $\rho_0 = I_z + F_z$, where $I_z = I_{1z}$ is the spin of the methine group and $F_z = I_{2z} + I_{3z} + I_{4z}$ denotes the three spins in the methyl group of lactate. During the pulse sequence the spins develop under the influence of the chemical shift, J-couplings, B_0 inhomogeneity and RF pulses. For ideal pulses, the first CH_3-selective $\frac{\pi}{2}$-pulse (P_1 in Fig. 1) generates y-magnetization for the methyl spins: $\rho_1 = I_z - F_y$. P_1 is followed by the delay τ. During the delays the spins evolve under the Hamiltonian

$$\mathcal{H} = \omega_{CH_3} F_z + \omega_{CH} I_z + 2\pi J I_z F_z + \omega_{B_0}(I_z + F_z),$$

where ω_{CH_3} and ω_{CH} denote the chemical shifts of the methyl and methine group, respectively. $J = 6.9$ Hz is the J-coupling between the methyl and methine spins. The last term in the Hamiltonian describes the effect of the inhomogeneity of the static magnetic field: $\omega_{B_0}(\vec{r})$ is the frequency shift as a function of the position $\vec{r}$. The delay $\tau = \frac{1}{2J}$ generates antiphase magnetization: $\rho_2 = I_z + 2I_zF_x$. Here we use a reference frame where the CH-spins are on resonance and disregard the chemical shift evolution of the CH_3-spins, since it is subsequently refocused by the 180°-pulse P_3. The effect of the magnetic field inhomogeneity ω_{B_0} is considered below. The following pulse P_2 rotates the methine spin and creates zero- and double-quantum coherences in $\rho_3 = -I_y - 2I_yF_x$. The single-spin term I_y in ρ_3 does not pass through the DQF and will not be considered in the following. The density operator ρ_3 represents a superposition of zero- and double-quantum coherences: $\rho_3 = \frac{1}{2i}(I^-F^- - I^+F^+ - I^+F^- + I^-F^+)$. The last two terms in ρ_3 are zero-quantum coherences which are eliminated by the filter and will therefore not be considered any further. The remaining terms are $\rho_3 = \frac{1}{2i}(I^-F^- - I^+F^+) = -I_yF_x - I_xF_y$. During the delay t_1, the gradient g_1, together with g_2, selects specific coherence pathways. The selective π-pulse P_3 refocuses couplings, chemical shift evolution and the evolution due to B_0-inhomogeneity for the CH_3-spins during t_1. However, the evolution of the methine spins under the B_0-inhomogeneity is not refocused and leads to $\rho_4 = (-I_yF_x + I_xF_y)\cos(\omega_{B_0}t_1) + (I_xF_x + I_yF_y)\sin(\omega_{B_0}t_1)$ at the end of the delay t_1. The pulse P_4 converts part of the double-quantum coherence back to antiphase magnetization. The detectable terms of the resulting density operator are $\rho_5 = -I_zF_x\cos(\omega_{B_0}t_1) + I_zF_y\sin(\omega_{B_0}t_1)$. During the following delay τ the evolution under the J-coupling generates again inphase magnetization for the methyl spins: $\rho_6 = -\frac{1}{2}(F_y\cos(\omega_{B_0}t_1) + F_x\sin(\omega_{B_0}t_1))$. Due to the inhomogeneity of B_0, the resulting magnetization has an inhomogeneous phase factor and the resulting signal is reduced to the spatial average. If the magnetization is allowed to precess for an additional period t_1, the magnetic field inhomogeneity refocuses and the signal increases, as shown in Fig. 2. However, during this additional delay, the methyl magnetization also evolves under the J-coupling,

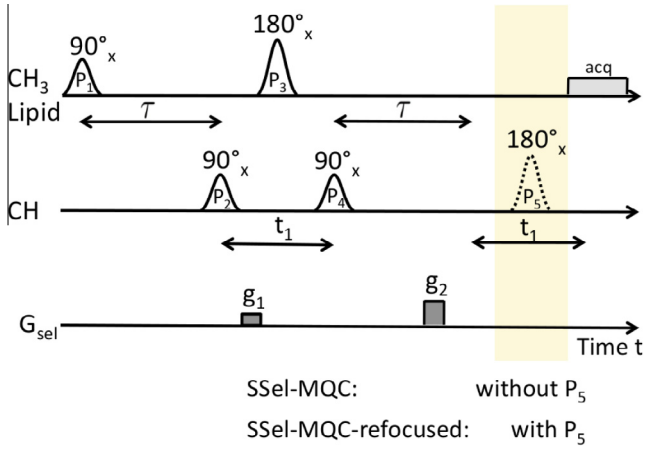

Fig. 1. Pulse sequence SSel-MQC [7] (without P_5) and refocused version SSel-MQC-refocused (with additional π-pulse P_5). The relative amplitudes of the selection gradients (G_{sel}) are g_1:g_2 = 1:2. The pulses in the first row (P_1 and P_3) are selective for the lactate methyl resonance at 1.3 ppm; the pulses in the second row (P_2, P_4 and P_5) excite the frequencies at 4.1 ppm (lactate methine group).

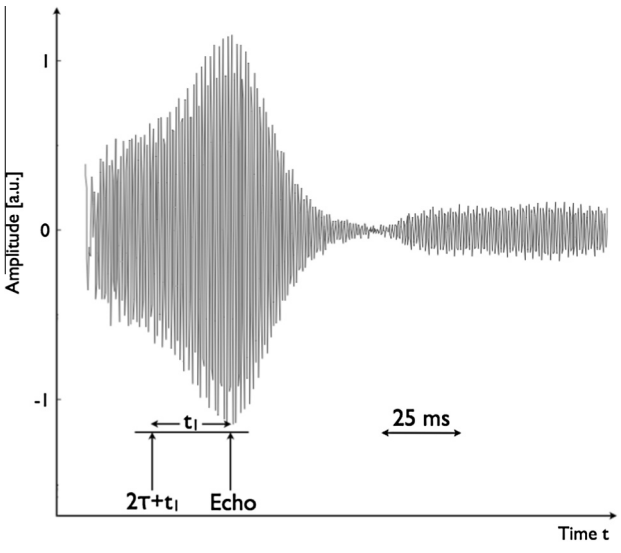

Fig. 2. Measured lactate methyl signal using the pulse sequence SSel-MQC in a phantom at 7 T. The data acquisition begins here before the anticipated time of the echo. The delay t_1 was 25 ms in this acquisition. The shift of the echo to the time ($2\tau + 2t_1$) is clearly visible. As described in the text the J-coupling and the chemical shift of the lactate spins are refocussed after different times which leads to a shift of the echo.

which converts the signal again into antiphase magnetization: $\rho_{7,unref} = -\frac{1}{2}F_y \cos(\pi J t_1)$. The J-coupling and the magnetic field inhomogeneity are thus refocused at different times, as shown in Fig. 2.

The displayed data were measured in a phantom in a 7 T MRI scanner. The whole FID was first Fourier transformed and all frequencies other than the lactate methyl region were set to zero. The lactate signal was then inversely Fourier transformed to obtain the pure lactate methyl time domain data.

2.2. Refocused SSel-MQC

The modulation of the lactate inphase signal with $\cos(\pi J t_1)$ in $\rho_{7,unref}$ can result in a large signal loss, depending on the value of t_1. This signal loss can be avoided by applying additional refocusing pulses. Boer et al. [8] used two CH-selective π-pulses in the first delay t_1 before and after the pulse P_3 in Fig. 1. Here, we show that the same result can be achieved by applying a single refocusing pulse to the CH-spins, which is placed in the middle of the last delay t_1 (see Fig. 1). The density operator at the end of the sequence is then refocused to $\rho_{7,refoc} = -\frac{1}{2}F_y$: the chemical shift, the effect of the B_0-inhomogeneity as well as the J-coupling are completely refocused and a maximal lactate signal is formed.

3. Materials and methods

The experimental tests were performed on two different devices: (a) on a high-resolution NMR spectrometer and (b) on a 7 T whole-body MRI scanner. For the NMR measurements a Bruker Avance II 500 MHz NMR spectrometer with a Bruker QXI high-resolution probehead was used. The phantom was a 5 mm sample tube containing lactate in D_2O. The measurements in (b) were performed on a Magnetom 7 T Siemens MRI scanner equipped with a self-built 8-channel head coil based on [21]. The phantom used was a spherical glass vessel with a diameter of 7 cm containing the metabolites lactate and alanine in a mixture of D_2O and H_2O. Spectra were acquired with the sequences SSel-MQC and SSel-MQC-refocused. In (a) and (b) spectra were acquired from the whole phantom, i.e. no localization method was applied. The spectra in (b) were postprocessed with the programm JMRUI. The applied steps were truncation, zero filling and apodization. The processed spectra were evaluated quantitatively in MATLAB by fitting Lorentzian lines to the data.

4. Results

As discussed in Section 2, the excitation sequence SSel-MQC leads to a modulation of the signal with the factor $cos(\pi J t_1)$ and therefore to a reduction of the overall signal. Fig. 3 shows a stacked plot of spectra aquired with SSel-MQC in a phantom at 7 T using different delays t_1. The shortest accessible t_1 delay on this machine was 25 ms, which corresponds to $\cos(\pi J t_1) \approx 0.85$, corresponding to a signal reduction by 15%. As shown in Fig. 3, the loss grows rapidly with increasing t_1: the inphase magnetization of lactate-CH_3 vanishes gradually and at the same time the antiphase signal grows. In the spectrum with $t_1 = 70$ ms almost maximal antiphase magnetization can be seen. Here the amplitude of the inphase magnetization is close to zero.

For *in vivo* measurements in lipid-rich tissues a longer t_1 delay may become necessary because the gradients g_1 and g_2 need to be strong enough to completely dephase the lipid signal. In the case that the maximal gradient amplitudes are reached this means that the duration of g_1 and g_2 needs to be longer, implying in turn longer t_1 delays, as shown by Boer et al. [8]. t_1 values in the range of 30–60 ms appear to be required for satisfactory lipid signal suppression [8]. Fig. 3 clearly shows that with the original SSel-MQC

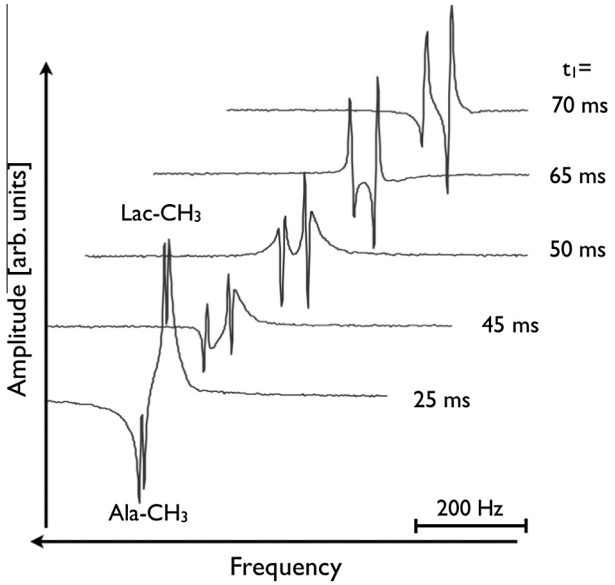

Fig. 3. Stacked plot of the edited unrefocused spectra (phase-corrected real part) using the sequence SSel-MQC with different lengths of the evolution period t_1 measured in a phantom at 7 T. The displayed spectral region shows the lactate and alanine methyl resonances. The desired inphase lactate signal is modulated with $cos(\pi J t_1)$ and the antiphase contribution gradually rises for longer t_1 delays.

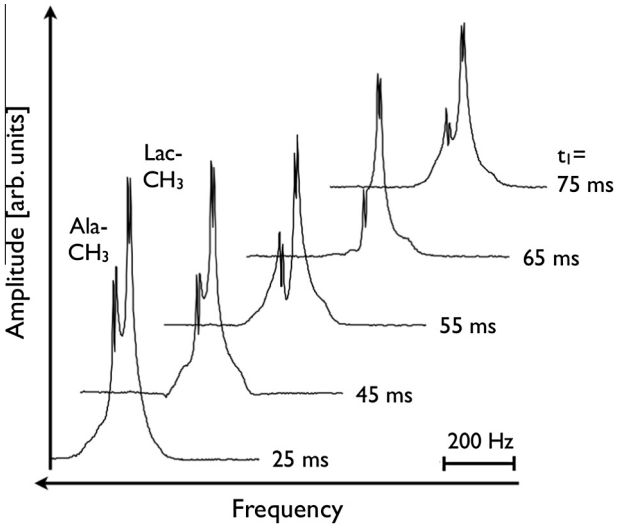

Fig. 4. Stacked plot of the edited refocused spectra (absolute value) using the sequence SSel-MQC-refocused with different lengths of the evolution period t_1 measured in a phantom at 7 T. The displayed spectral region shows the lactate and alanine methyl resonances. Even for long delays t_1, such as e.g. $t_1 = 75$ ms, the detected lactate signal still has a high amplitude.

sequence in this region of t_1 values only a very small lactate inphase signal is left, which is overlayed by a considerable amount of antiphase signal. Furthermore, the contribution of a strong antiphase signal complicates the quantification because the fitting of Lorentzian line shapes to a superposition of inphase and antiphase signals is more challenging. In addition, the antiphase signal suffers from signal cancellation unless the linewidth is very small.

The refocused excitation scheme introduced in Section 2.2 eliminates the J-modulation and restores the signal lost due to dephasing.

Fig. 4 shows a series of spectra acquired with the SSel-MQC-refocused sequence. The spectra clearly demonstrate that the undesired J-modulation of the signal has been eliminated and pure

inphase lactate methyl signals can be acquired which simplifies the quantification of the metabolite content. The amplitude of the lactate methyl signal is still relatively high even for t_1 delays as long as 75 ms. Therefore, the refocused sequence makes a quantitative determination of the lactate content possible even in situations where long gradient durations for g_1 and g_2 are required.

For a quantitative evaluation of the sequence performance, Fig. 5 compares the signal amplitudes for the two sequences SSel-MQC and SSel-MQC-refocused measured on both instruments. The signal amplitudes for the MRI scanner measurements were determined by applying the standard postprocessing of the data in JMRUI and subsequently fitting the real parts of the spectra in MATLAB. For the refocused spectra a superposition of two inphase doublets (for lactate and alanine) was fitted to the data. In the case of the unrefocused spectra a superposition of an inphase doublet and an antiphase doublet for each lactate and alanine was used for fitting. With the data from the fit a quantitative evaluation of the pure inphase lactate-CH_3 signal without overlapping alanine or antiphase components is possible. The results are shown in Fig. 5. The refocused version of the sequence excites, in accordance with the theory, a large lactate methyl inphase signal (blue squares) where signal loss comes only from T_2 decay. The solid blue curve is a fitted T_2 decay ($A \cdot \exp(-(2\tau + 2t_1)/T_2)$). The data from the unrefocused sequence (black triangles) match the theoretically predicted behaviour as shown by the black dashed curve, which corresponds to a T_2 decay multiplied by $cos(\pi J t_1)$. For a t_1 value of e.g. 50 ms the refocused version gives a signal that is twice as large as the unrefocused version. For $t_1 = 70$ ms even a four times larger signal is reached. Similar experiments and evaluations were additionally performed on a 500 MHz NMR spectrometer. The results are also displayed in Fig. 5. The data points represent the integrated lactate methyl doublet. For the unrefocused sequence SSel-MQC and for SSel-MQC-refocused, as described in Fig. 1, the dependence of the lactate methyl signal on the t_1 values is analogue to the observed behaviour at 7 T.

Fig. 6 shows a direct comparison of the resulting spectra for $t_1 = 50$ ms, which clearly shows the large signal gain resulting from the refocusing. In addition, the line shape shows that the unrefocused spectrum does not contain a pure inphase signal and quantification will be more complicated in that case. The chosen value of $t_1 = 50$ ms is a realistic value for *in vivo* measurements of lactate in a lipid-rich environment [8] like breast or muscle.

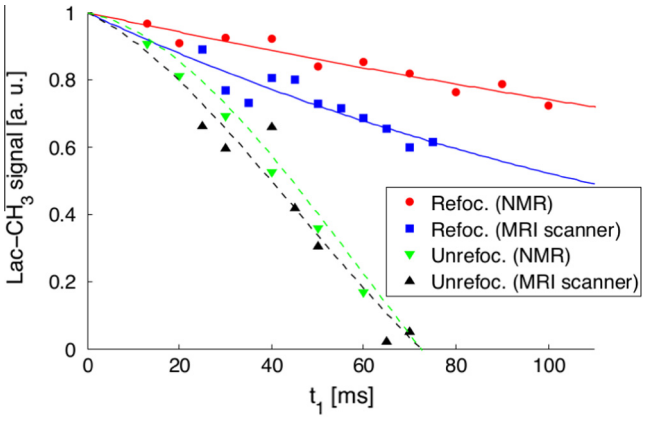

Fig. 5. Dependance of the lactate methyl inphase signal on the length of the evolution period t_1 for the pulse sequences SSel-MQC and SSel-MQC-refocused measured on a phantom at 7 T and at a 500 MHz NMR-spectrometer. The original SSel-MQC sequence produces a signal that is modulated with $cos(\pi J t_1)$ (black and green triangles). With the refocused multiple-quantum filter the full signal can be reobtained (red circles and blue squares). The signal is only diminished by the loss due to T_2 decay. The solid lines represent a fit of an exponential decay to the data. The dashed curves were obtained by multiplying these fits with $cos(\pi J t_1)$ respectively. (For interpretation of the references to colour in this figure legend, the reader is referred to the web version of this article.)

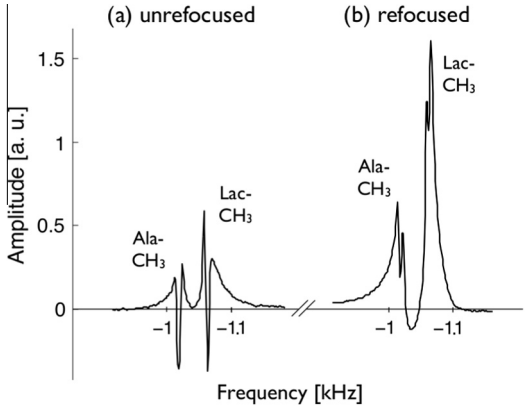

Fig. 6. Direct comparison of the edited spectra (phase-corrected real part) measured with the sequence SSel-MQC (a) and SSel-MQC-refocused (b) at 7 T for t_1 = 50 ms.

For comparison, we also tested the recently proposed sequence of Boer et al. [8] on the NMR spectrometer. In contrast to our sequence, which uses a single refocusing pulse, the sequence proposed by Boer et al. relies on two refocusing pulses. We found that for t_1 delays up to approx. 60–70 ms the performance of the two sequences is identical within the measurement uncertainty.

Fig. 7 shows the simulated dependence of the lactate methyl signal on a miscalibration of the RF amplitude. The curves were calculated with MATLAB for different t_1 values, assuming an ideal B_0 field without inhomogeneity. For this situation the simulated curves represent the behaviour of both SSel-MQC and SSel-MQC-refocused at the same time. As can be seen in the figure an additional problem occurs for long t_1 delays in the presence of RF inhomogeneity: sequences with long t_1 delays are significantly more sensitive to RF inhomogeneity. As an example, a sequence with $t_1 = 60$ ms and RF miscalibration of ±30% from the ideal value yields only ≈50% of the lactate signal compared to a sequence with $t_1 = 13$ ms. This represents an additional reason why the t_1 delay should be kept as short as possible. With the refocused multiple-quantum filter with one refocussing pulse, as described in Fig. 1, a shorter t_1 delay can be used than in the version with two refocussing pulses.

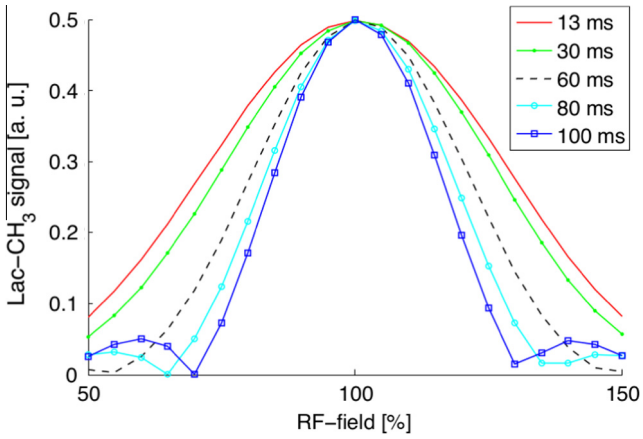

Fig. 7. Simulation of the dependance of the lactate methyl signal for the sequence SSel-MQC on miscalibration of the RF amplitude for different t_1 values calculated with MATLAB. An RF-field of 100% corresponds to the nominal RF amplitude.

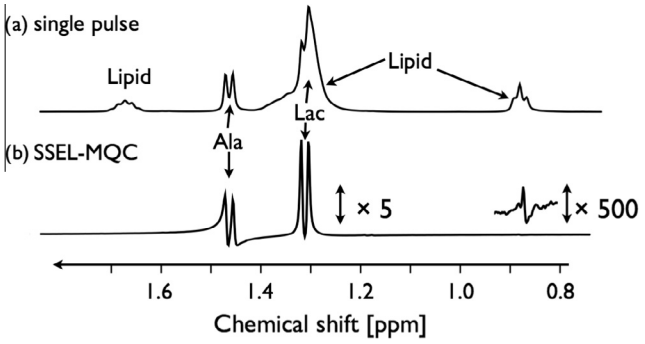

Fig. 8. Experimental spectra of a sample containing lactate, alanine and lipid. (a) Reference spectrum obtained with a hard 90°-pulse. (b) Spectrum obtained with the SSel-MQC sequence using Gaussian pulses. The lipid suppression is performed very well by the selection gradients. The lipid signals are suppressed by a factor 450.

5. Discussion and conclusion

Lactate editing with the multiple-quantum filter sequence SSel-MQC originally developed by He et al. [7] suffers from the drawback that the desired lactate inphase signal is reduced by a factor $\cos(\pi J t_1)$ that depends on the evolution time t_1. In lipid-rich tissues, where the t_1 delays have to be chosen longer than 30 ms to achieve sufficient suppression [8], this modulation results in a significant signal loss.

The refocused version of the multiple-quantum filter presented in this work avoids this signal loss. The refocussing is done by an additional 180°-pulse in the last delay t_1. As a result the pure inphase lactate methyl signal is restored. The remaining signal loss is due to (homogeneous) T_2 relaxation.

In this study, we showed by analytical calculation and experimental verification on an NMR spectrometer and a 7 T MRI scanner the effect of the refocussing. A significantly higher lactate signal can be acquired, and, therefore, lactate editing using long delays t_1 in lipid-rich environments becomes possible. A comparison with the refocused multiple-quantum filter seqence from Boer et al. [8] shows that the refocussing with one and with two additional 180°-pulses works identically up to t_1 values of 60–70 ms. The advantage of the refocused sequence with a single 180°-pulse as presented in this work is a lower additional SAR contribution from only one, instead of two additional 180°-pulses. Furthermore, the delay t_1 can be kept shorter with the refocused sequence presented here because there is no need to place two additional 180°-pulses in the first delay t_1. In addition, simulations show that the SSel-MQC sequence with long t_1 delays is substantially more sensitive to RF inhomogeneity. Therefore, a short delay t_1 helps to make the sequence as robust as possible in the presence of RF inhomogeneity.

The SSel-MQC sequence has a very good performance in the suppression of lipid signals, as shown in Fig. 8. The additional 180°-pulse P_5 does not affect the ability of the sequence to suppress strong lipid signals. The pulse P_5 in the last part of the sequence is only selective for the lactate methine spins. The lipid signal is not excited by this additional pulse. The lipid suppression is accomplished by the selection gradients g_1 and g_2 and works very well, as shown in Fig. 8. Therefore the optimized sequence SSel-MQC-refocused suppresses the lipid signal just as well as the original sequence SSel-MQC.

We described here a refocused multiple-quantum filter for selective excitation of lactate signals. The principle of this refocussing can equally be applied to MQ-filters for selective excitation of other metabolites in different applications.

As an outlook, the refocused multiple-quantum filter described above might be combined with optimized robust pulses (see Holbach et al. [22]) to minimize effects of B_0 and RF inhomogeneity for applications in MRI scanners. As the next steps, we therefore plan to implement the refocused and optimized sequence for *in vivo* studies.

References

[1] S.-C. Lee, H. Poptani, S. Pickup, W.T. Jenkins, S. Kim, C.J. Koch, E.J. Delikatny, J.D. Glickson, Early detection of radiation therapy response in non-Hodgkin's lymphoma xenografts by in vivo ^{1}H magnetic resonance spectroscopy and imaging, NMR Biomed. 23 (6) (2010) 624–632.
[2] R.A. de Graaf, D.L. Rothman, In vivo detection and quantification of scalar coupled ^{1}H NMR resonances, Concepts Magn. Reson. 13 (1) (2001) 32–76.
[3] R.A. de Graaf, D.L. Rothman, Detection of γ-Aminobutyric Acid (GABA) by longitudinal scalar order difference editing, J. Magn. Reson. 152 (1) (2001) 124–131.
[4] M.A. Smith, J.A. Koutcher, K.L. Zakian, J-difference lactate editing at 3.0 Tesla in the presence of strong lipids, J. Magn. Reson. Imaging 28 (6) (2008) 1492–1498.
[5] C. Choi, N.J. Coupland, S. Kalra, P.P. Bhardwaj, N. Malykhin, P.S. Allen, Proton spectral editing for discrimination of lactate and threonine 1.31 ppm resonances in human brain in vivo, Magn. Reson. Med. 56 (3) (2006) 660–665.
[6] H. Hetherington, J. Hamm, J. Pan, D. Rothman, R. Shulman, A fully localized ^{1}H homonuclear editing sequence to observe lactate in human skeletal muscle after exercise, J. Magn. Reson. (1969) 82 (1) (1989) 86–96.
[7] Q. He, D.C. Shungu, P.C.M.V. Zijl, Z.M. Bhujwalla, J.D. Glickson, Single-scan in vivo lactate editing with complete lipid and water suppression by Selective Multiple-Quantum-Coherence Transfer (Sel-MQC) with application to tumors, J. Magn. Reson. 106 (1995) 203–211.
[8] V.O. Boer, P.R. Luijten, D.W.J. Klomp, Refocused double-quantum editing for lactate detection at 7 T, Magn. Reson. Med. 69 (1) (2012) 1–6.
[9] S. Pickup, S. Lee, A. Mancuso, J. Glickson, Lactate imaging with Hadamard-encoded slice-selective multiple quantum coherence chemical shift imaging, Magn. Reson. Med. 60 (2) (2008) 299–305.
[10] G. Melkus, P. Mörchel, V.C. Behr, M. Kotas, M. Flentje, P.M. Jakob, Short-echo spectroscopic imaging combined with lactate editing in a single scan, NMR Biomed. 21 (10) (2008) 1076–1086 (ISSN 1099-1492).
[11] R. Hurd, D. Freeman, Metabolite specific proton magnetic resonance imaging, Proc. Nat. Acad. Sci. 86 (12) (1989) 4402–4406.
[12] R. Hurd, D. Freeman, Proton editing and imaging of lactate, NMR Biomed. 4 (2) (1991) 73–80.
[13] J.M. Star-Lack, D.M. Spielman, Zero-quantum filter offering single-shot lipid suppression and simultaneous detection of lactate, choline and creatine resonances, Magn. Reson. Med. 46 (6) (2001) 1233–1237.
[14] E.A. Mellon, S.-C. Lee, S. Pickup, S. Kim, S.C. Goldstein, T.F. Floyd, H. Poptani, E.J. Delikatny, R. Reddy, J.D. Glickson, Detection of lactate with a hadamard slice selected, selective multiple quantum coherence, chemical shift imaging sequence (HDMD-SelMQC-CSI) on a clinical MRI scanner: application to tumors and muscle ischemia, Magn. Reson. Med. 62 (6) (2009) 1404–1413.
[15] S.-C. Lee, M. Marzec, X. Liu, S. Wehrli, K. Kantekure, P.N. Ragunath, D.S. Nelson, E.J. Delikatny, J.D. Glickson, M.A. Wasik, Decreased lactate concentration and glycolytic enzyme expression reflect inhibition of mTOR signal transduction pathway in B-cell lymphoma, NMR Biomed. 26 (1) (2012) 106–114.
[16] H. Zhu, D. Rubin, Q. He, The fast spiral-SelMQC technique for in vivo MR spectroscopic imaging of polyunsaturated fatty acids in human breast tissue, Magn. Reson. Med. 67 (1) (2012) 8–19.
[17] G. Melkus, P. Mörchel, V.C. Behr, M. Kotas, M. Flentje, P.M. Jakob, Sensitive J-coupled metabolite mapping using Sel-MQC with selective multi-spin-echo readout, Magn. Reson. Med. 62 (4) (2009) 880–887.
[18] S. Thakur, J. Yaligar, J. Koutcher, In vivo lactate signal enhancement using binomial spectral-selective pulses in selective MQ coherence (SS-SelMQC) spectroscopy, Magn. Reson. Med. 62 (3) (2009) 591–598.
[19] S. Magnitsky, G.K. Belka, C. Sterner, S. Pickup, L.A. Chodosh, J.D. Glickson, Lactate detection in inducible and orthotopic Her2/neu mammary gland tumours in mouse models, NMR Biomed. 26 (1) (2012) 35–42.
[20] M. Muruganandham, J.A. Koutcher, G. Pizzorno, Q. He, In vivo tumor lactate relaxation measurements by selective multiple-quantum-coherence (Sel-MQC) transfer, Magn. Reson. Med. 52 (4) (2004) 902–906.
[21] S. Orzada, O. Kraff, L.C. Schäfer, I. Brote, A. Bahr, T. Bolz, S. Maderwald, M.E. Ladd, A.K. Bitz, 8-channel transmit/receive head coil for 7 T human imaging using intrinsically decoupled strip line elements with meanders, in: ISMRM 17th Annual Meeting Honolulu, Hawaii, 2009.
[22] M. Holbach, J. Lambert, D. Suter, Optimized multiple-quantum filter for robust selective excitation of metabolite signals, J. Magn. Reson. 243 (C) (2014) 8–16.